Theoretical Ingredients for Tuning Thermoelectric Properties of Semiconducting Materials

G P Srivastava
Physics, University of Exeter

TE workshop 15 Feb 2017

Outline of talk

- Brief discussion on ZT
- The PGEC concept
- Theoretical ingredients for computation of ZT
- Phonon engineering of thermoelectric nanocomposite semiconductors
- Some results
- Summary

The main concern of the TE community:

TE generation efficiency η
TE cooling performance Φ
Figure of merit ZT

$T_c(T_h)$ = temperature of cold(hot) end of device

$$\eta_{TE} = \frac{T_h - T_c}{T_h} \frac{\sqrt{1+ZT} - 1}{\sqrt{1+ZT} + \frac{T_c}{T_h}},$$

$$\Phi_{TE} = \frac{T_c}{T_h - T_c} \frac{\sqrt{1+ZT} - \frac{T_h}{T_c}}{\sqrt{1+ZT} + 1}.$$

Efficiency for T_c=300K and T_h=700K
13% for ZT=1; 19% for ZT=2;
24% for ZT=3; 27% for ZT=4

An inconvenient truth about thermoelectrics

Cronin B. Vining

Nature Materials 8, 83 (2009)

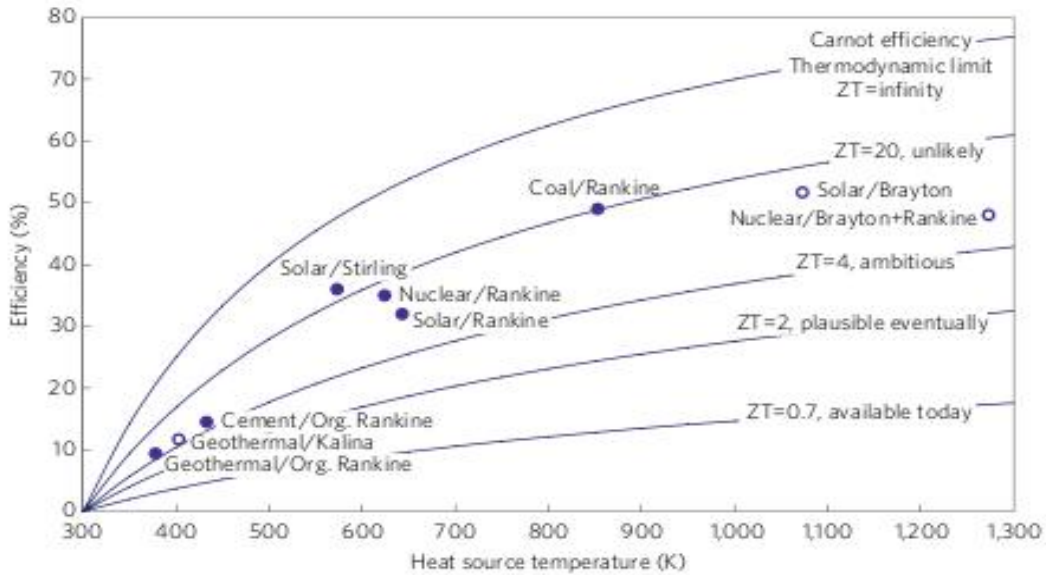

Figure 2 | Assessing thermoelectrics. Efficiency of 'best practice' mechanical heat engines compared with an optimistic thermoelectric estimate (see main text for description).

Despite recent advances, thermoelectric energy conversion will never be as efficient as steam engines. That means thermoelectrics will remain limited to applications served poorly or not at all by existing technology. Bad news for thermoelectricians, but the climate crisis requires that we face bad news head on.

Material type and components of ZT

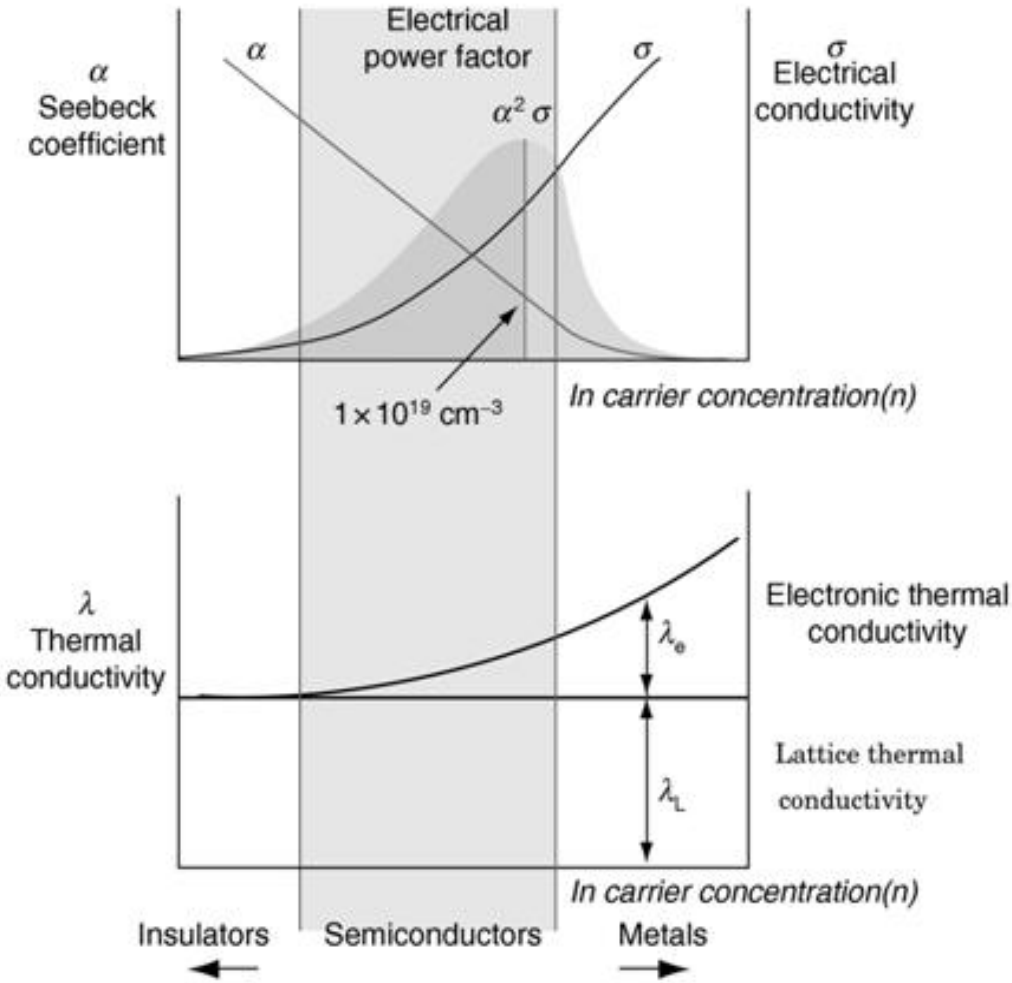

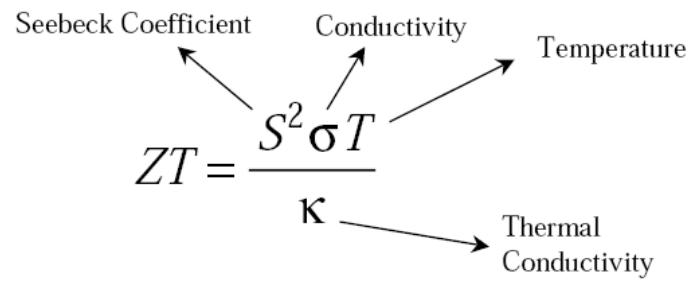

Doped semiconducting materials good candidates for high ZT

Current status

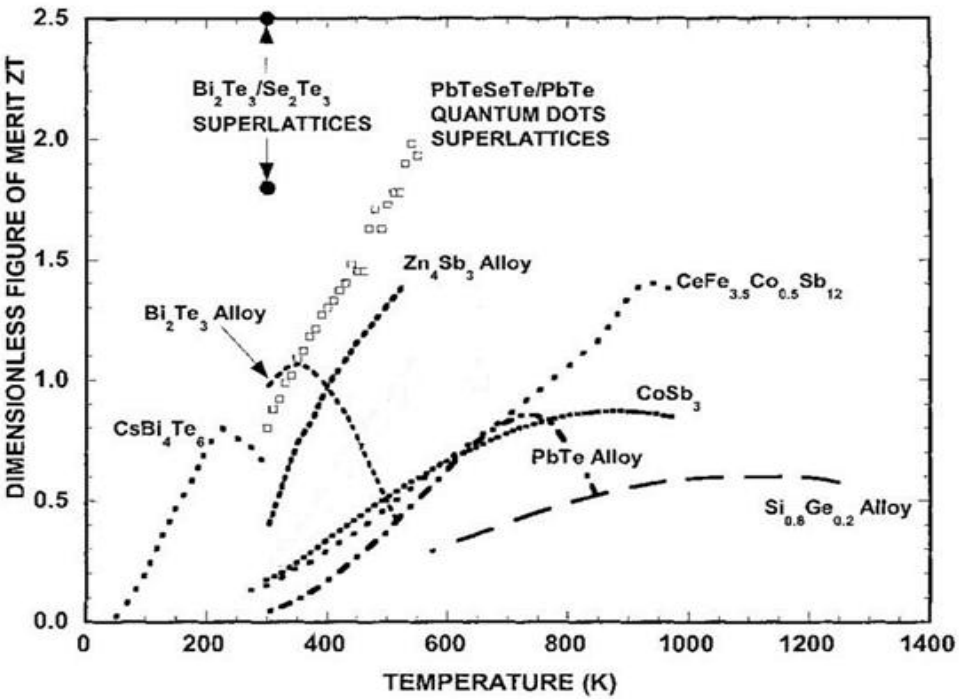

G. Chen, M.S. Dresselhaus,Int. Mat. Rev., **48**, (2003).

Reminder:
Efficiency for T_c=300K and T_h=700K
13% for ZT=1; 19% for ZT=2;
24% for ZT=3; 27% for ZT=4

Message from previous slide and other works

Research over 6 decades (1950-2010) suggests:

Large ZT for bulk alloys or complex crystal structure

Larger ZT for embedded structures

ZT>4 for commercial viability

fabricating ordered nano-composite structures,

e.g. (a) superlattice formation;

(b) embedded wire formation,

(c) embedded dot formation

Another look at the expression for ZT

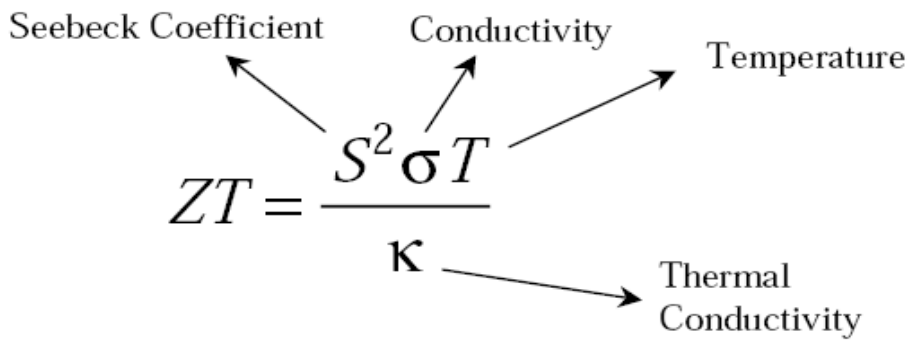

$S = S(\text{carriers})$

$\sigma = \sigma(\text{carriers})$

$\kappa = \kappa_{el} + \kappa_{ph}$

$\kappa_{el} = \kappa_{el}(\text{mono-polar}) + \kappa_{el}(\text{bi-polar})$

ZT determined by a total of 5 transport coefficients.

While other coeffs are inter-related,

phonon conductivity K_{ph} can be controlled independently

Limits of thermal transport

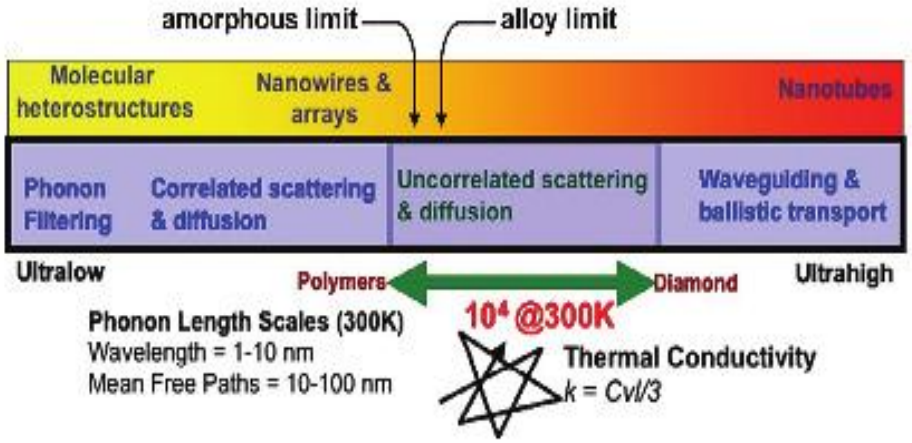

Fig. 1 Schematic illustrating various approaches to expand the limits of thermal transport. This can be accomplished with nanostructured materials, which can tune into the phonon wavelength and mean free path.

Kim et al, Nanotoday 2, 40 (2007)

K_{ph} spans four orders of magnitude

Promise land: the PGEC concept

- $ZT \propto S^2\sigma/k_{ph} \propto \mu m^{*3/2}/k_{ph}$ (μ: carrier mobility)

- Conficting requirements of high m* and high μ can be by met by employing the PGEC (phonon-glass electron-crystal) concept: achieve record low K_{ph} without appreciable deterioration in electron transport (Slack 1994).

- For low K_{ph} fabricate nanocomposite structures, with length scale range 5-250 nm, with deliberately roughened (or intermixed) interfaces.

Theoretical ingredients-1

Carrier transport:

$$(L_{\mathrm{EE}})_{ij} = Q^2 \sum_k v_k^i v_k^j \tau_k \frac{\partial \bar{f}_k}{\partial E_k}, \tag{17}$$

$$(L_{\mathrm{ET}})_{ij} = \frac{Q}{T} \sum_k v_k^i v_k^j \tau_k (E_k - E_{\mathrm{F}}) \frac{\partial \bar{f}_k}{\partial E_k}, \tag{18}$$

$$(L_{\mathrm{TT}})_{ij} = \frac{1}{T} \sum_k v_k^i v_k^j \tau_k (E_k - E_{\mathrm{F}})^2 \frac{\partial \bar{f}_k}{\partial E_k}, \tag{19}$$

where $Q = -e(e)$ is the carrier [electron(hole)] charge, $\boldsymbol{k}$ represents the carrier wavevector, $v_k^i = \frac{\partial E_k}{\partial k_i}$ is the ith component of the carrier velocity, τ_k is the carrier relaxation time, $E_{\mathrm{F}} \equiv E_{\mathrm{F}}(T)$ represents the Fermi level and $\bar{f}_k$ is the Fermi–Dirac equilibrium distribution function. With these, the carrier components of the transport coeffcients can be expressed as

$$\sigma_{ij} = (L_{EE})_{ij}, \tag{20}$$

$$S_{ij} = -(L_{EE}^{-1})_{il}(L_{ET})_{lj}, \tag{21}$$

$$(\kappa_{\mathrm{carriers}})_{ij} = (L_{EE}^{-1})_{il}(L_{ET})_{lk}(L_{TE})_{kj} - (L_{TT})_{ij}. \tag{22}$$

Theoretical ingredients-2

Phonon transport

Considerations must be based on phonon MFP (Λ) vs. unit cell size (d) in structure:

(1) $d \ll \Lambda$ (bulk and ultra-thin nanocomposites)
(2) $d \sim \Lambda$
(3) $d \gg \Lambda$

Theoretical ingredients-3

Phonon transport

(1) d << Λ (bulk and ultra-thin nanocomposites)

$$\kappa_{ij} = \frac{\hbar^2}{N_0 \Omega k_B T^2} \sum_{\boldsymbol{q},s} \omega^2(\boldsymbol{q}s) v_i(\boldsymbol{q}s) v_j(\boldsymbol{q}s) \tau(\boldsymbol{q}s) \bar{n}(\boldsymbol{q}s)(\bar{n}(\boldsymbol{q}s)+1),$$

N_0: No. of unit cells, Ω: Unit cell volume,

$\bar{n}$: Bose-Einstein distribution function,

$$\tau^{-1} = \tau_B^{-1} + \tau_{MD}^{-1} + \tau_{ID}^{-1} + \tau_{pp}^{-1}$$

τ_B^{-1}: boundary scattering,

τ_{MD}^{-1}: isotope scattering,

τ_{ID}^{-1}: interface scattering,

τ_{pp}^{-1}: phonon-phonon scattering,

$v_{\mathbf{q}s,i}$: i^{th} velocity component for phonon $\omega(\mathbf{q}s)$

Theoretical ingredients-4

Phonon transport in superlattices

(2) d ~ Λ and (3) d >> Λ

us consider a SL structure of repeat period size d_{SL}, containing material A of layer thickness d_A and material B of layer thickness d_B. The three regimes are:

[A] If $d_{SL} \gg \Lambda$, the cross-plane resistivity $1/\kappa_\perp$ will just be the weighted average of the bulk resistivities:

$$1/\kappa_\perp = \frac{1}{d_A + d_B}\left(\frac{d_A}{\kappa_A} + \frac{d_B}{\kappa_B}\right). \tag{144}$$

[B] If $d_{SL} \sim \Lambda$, the SL conductivity should be expressed as

$$1/\kappa_\perp = \frac{1}{d_A + d_B}\left(\frac{d_A}{\kappa_A} + \frac{d_B}{\kappa_B} + \frac{2}{\sigma_K}\right), \tag{145}$$

where σ_K is the Kapitza (boundary, or interface) conductance.

Theoretical ingredients-5

Phonon transport in low-fraction embedded nanowires and nanodots

Effective medium theory, based on multiple scattering theory

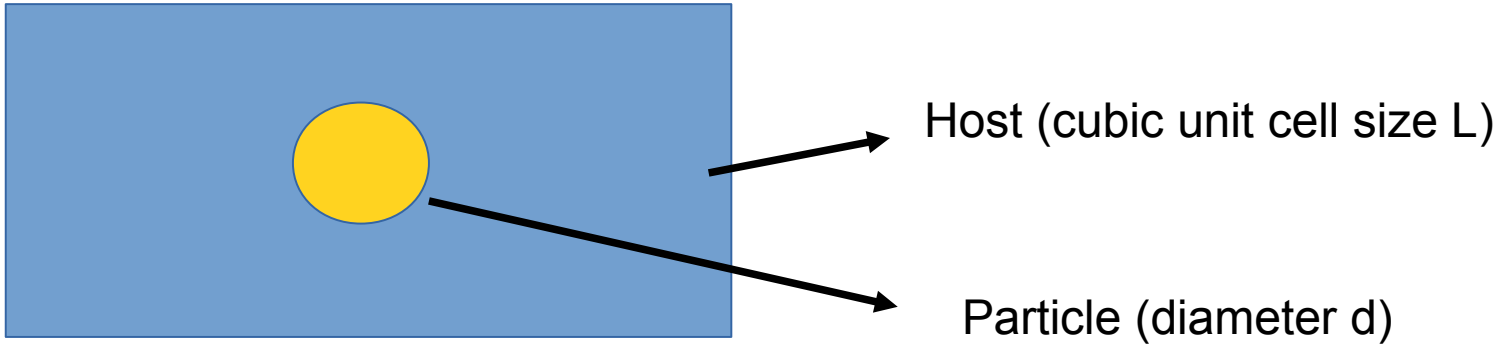

Nan et al, J. Appl. Phys. 81, 6692 (1997)
Minnich and Chen, Appl. Phys. Lett. 91, 073105 (2007)
Behrang et al, J. Appl. Phys. 114, 014305 (2013); Appl. Phys. Lett. 104, 063106 (2014)

Effective medium theory for particle insertion volume fraction V_f

Conductivity across particle-host interface: $K_\perp = g\, K_h$

Conductivity along particle-host interface: $K_\parallel = V_f\, K_p + (1-V_f)\, K_h$

$$\text{Nanodots}: \quad g = \frac{\kappa_p(1+2\alpha) + 2\kappa_h + 2V_f[\kappa_p(1-\alpha) - \kappa_h]}{\kappa_p(1+2\alpha) + 2\kappa_h - V_f[\kappa_p(1-\alpha) - \kappa_h]},$$

$$\text{Nanowires}: \quad g = \frac{\kappa_p(1+\alpha) + \kappa_h + V_f[\kappa_p(1-\alpha) - \kappa_h]}{\kappa_p(1+\alpha) + \kappa_h - V_f[\kappa_p(1-\alpha) - \kappa_h]},$$

$$\text{Superlattices}: \quad g = \frac{\kappa_p}{\kappa_p - V_f[\kappa_p(1-\alpha) - \kappa_h]},$$

K_p (K_h) : particle(host) conductivity; $\alpha = K_h\, R_{TBR}/(d/2)$

$R_{TBR} = 4\left(\frac{C_h v_h + C_p v_p}{C_h v_h C_p v_p}\right)$, = Kapitza's thermal boundary resistance

C=specific heat; v=sound speed

Effective medium theory for particle insertion volume fraction V_f

Particle interface density Φ plays an important role:

System	V_f	Φ
ND	$\frac{4\pi}{3}(\frac{r}{L_{cell}})^3$	$\frac{3}{r}V_f$
$NW_{\parallel}$	$\pi(\frac{r}{L_{cell}})^2\frac{L_w}{L_{cell}}$	$\frac{2}{L_w}V_f$
$NW_{\perp}$	$\pi(\frac{r}{L_{cell}})^2$	$\frac{2}{r}V_f$
$SL_{\perp}$	$\frac{L_{PbSe}}{L_{cell}}$	$\frac{V_f}{L_{PbSe}}$

Ingredients for computation of ZT

Power factor:

(1) Electronic band structure;
(2) Temperature dependent Fermi energy;
(3) Relevant carrier relaxation rates;
(4) Sound scheme for carrying out **k** momentum-space summation (integration).

Phonon transport:

(5) Phonon dispersion relations;
(6) Relevant phonon relaxation times;
(7) Kapitza thermal boundary resistance;
(8) Sound scheme for carrying out **q** momentum-space summation (integration).

SOME RESULTS

[1] Doped $Si_{0.75}Ge_{0.25}$ alloy ($n=9.4 \times 10^{25}\ m^{-3}$)

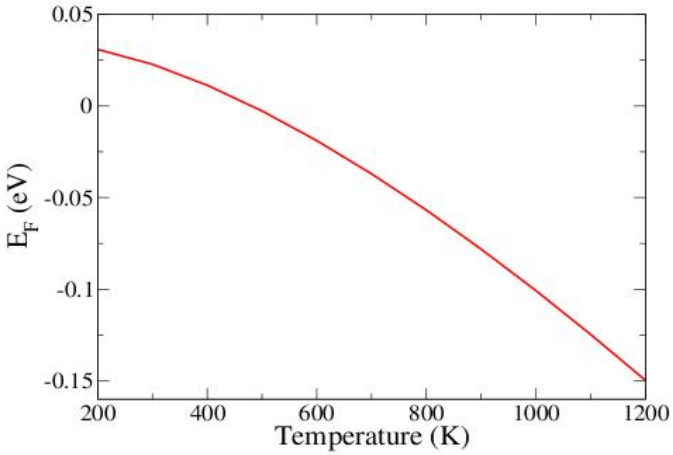

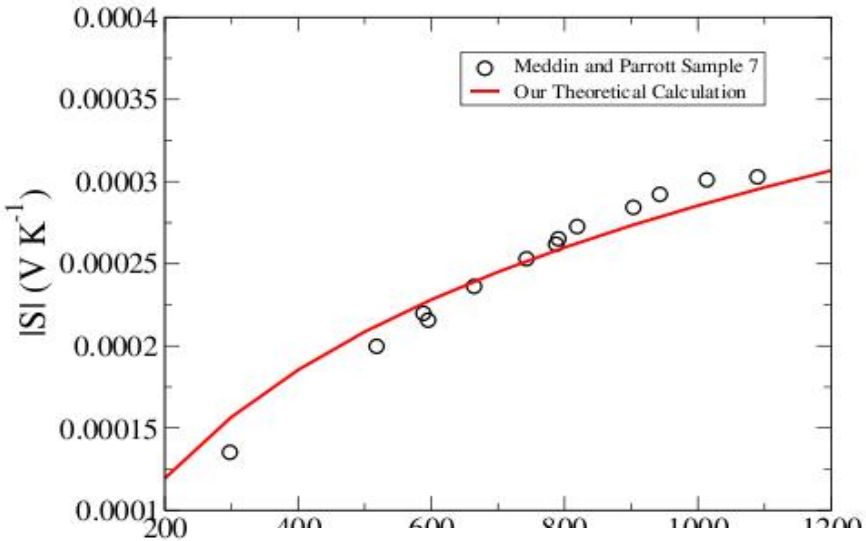

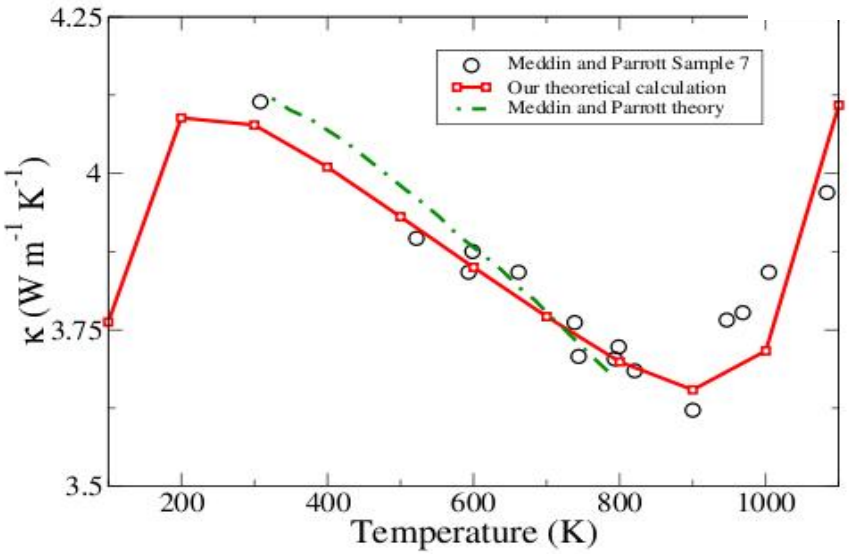

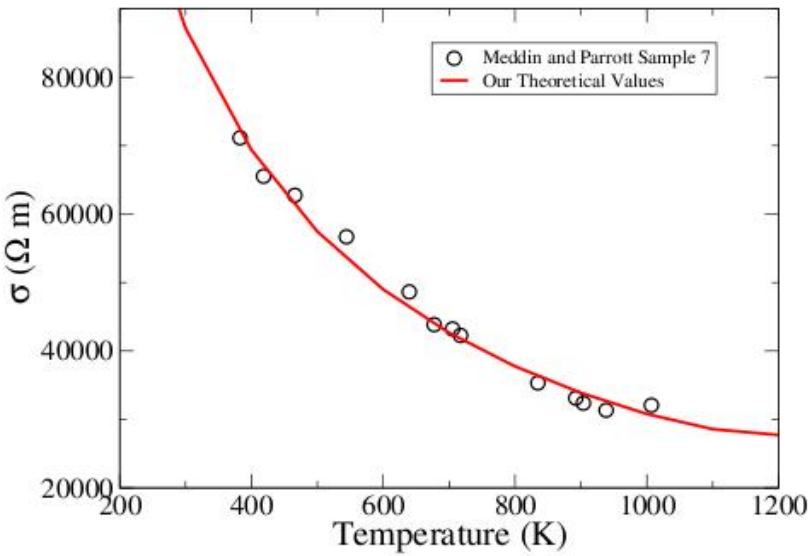

Thomas and Srivastava, PRB 86, 045205 (2012)

Doped $Si_{0.75}Ge_{0.25}$ alloy ($n=9.4 \times 10^{25}\ m^{-3}$)

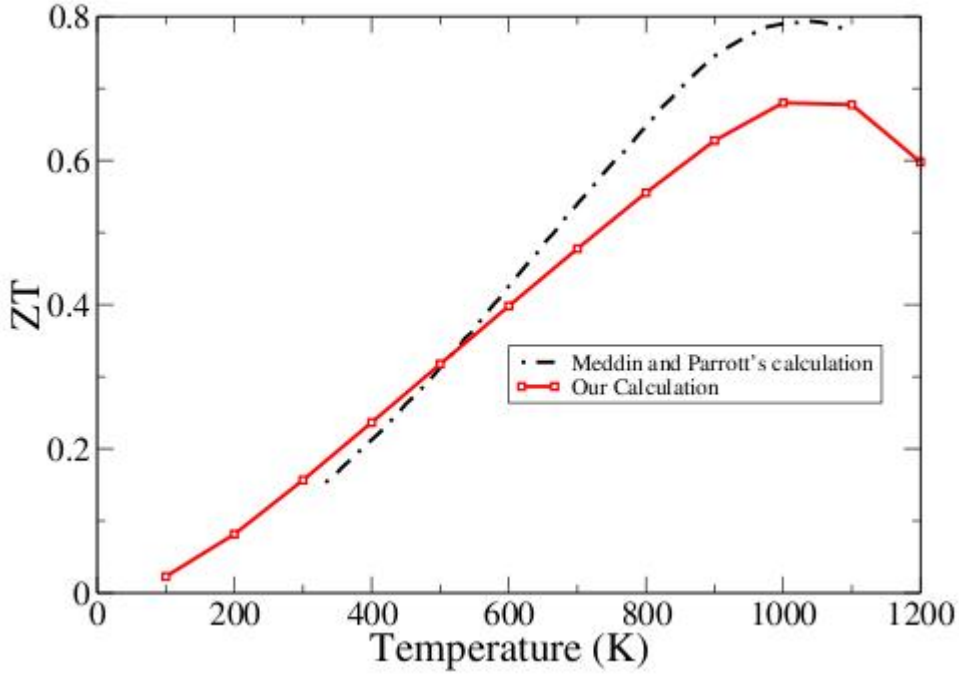

ZT < 1

Thomas and Srivastava, PRB 86, 045205 (2012)

[2] Ultra-thin superlattices: SiGe(4,4)

periodicity 2.2 nm; different doping levels and sample lengths

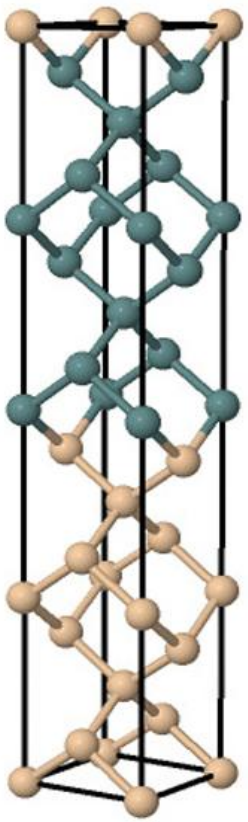

FIG. 1. Atomic structure representation of the Si(4)Ge(4)[001] SL. Gold and blue-gray spheres represent Si and Ge atoms, respectively. Figures were generated using Jmol.[57]

1 bilayer interface mixing

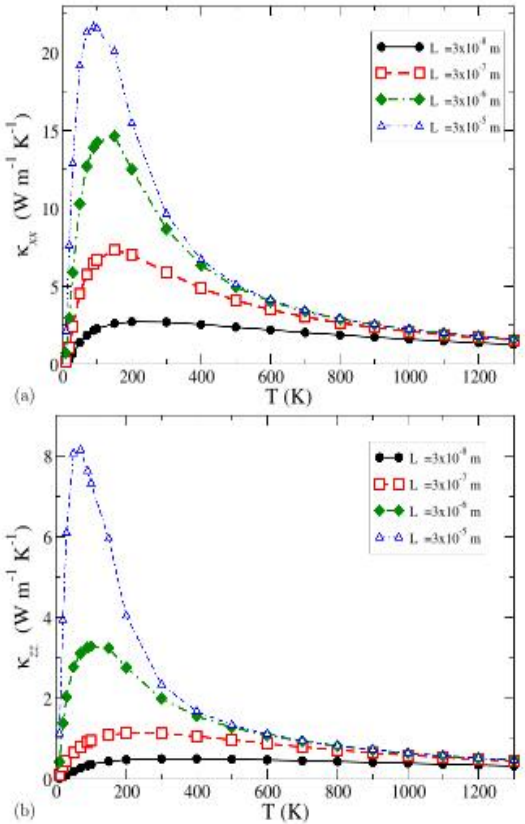

FIG. 5. Length dependence of phonon conductivity in the (a) x-direction and (b) z-direction for the (4,4) Si/Ge[001] superlattice with interface parameters $\alpha = 2.0$, $B = 1$, and $N_d = 10^{25}\,\mathrm{m}^{-3}$. (Results in the y-direction are similar to those in the x-direction.)

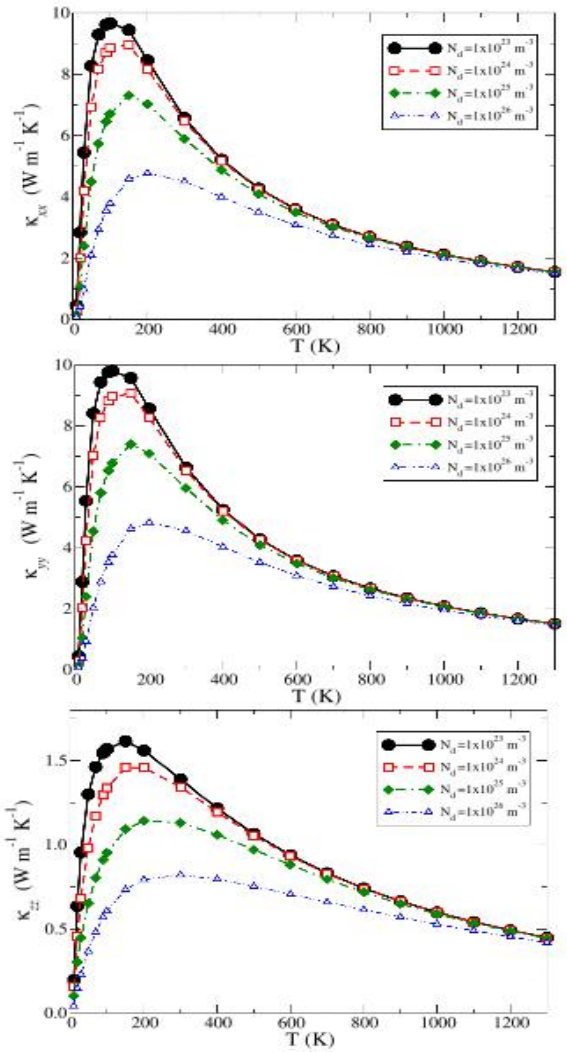

FIG. 3. Components of the lattice thermal conductivity tensor κ_{ph} for the Si(4)Ge(4)[001] superlattice when $L_B = 3 \times 10^{-7}$ m, $\alpha = 2.0$, and $B = 1.0$ (see text and Ref. 43 for notation).

Thomas and Srivastava, J Appl Phys 119, 244309 (2016)

Ultra-thin superlattices: SiGe(4,4)

periodicity 2.2 nm; 1 bilayer interface mixing; doping n=9.4 x10^{25} m^{-3}

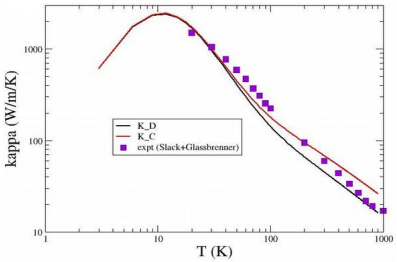

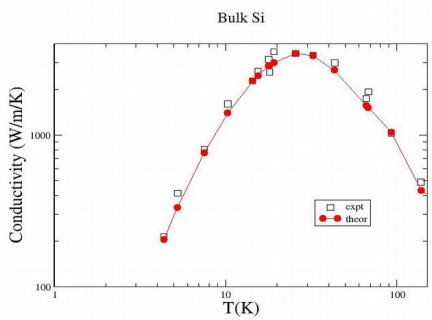

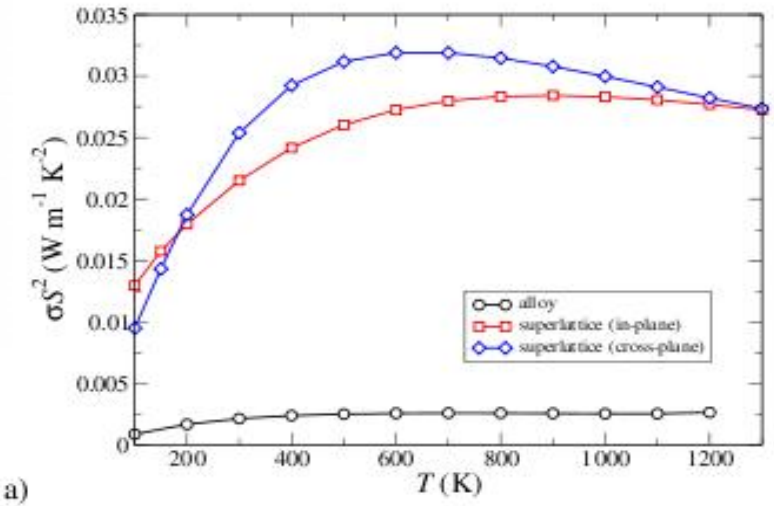

a)

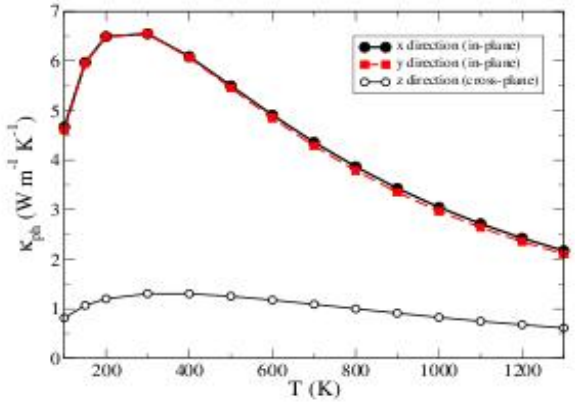

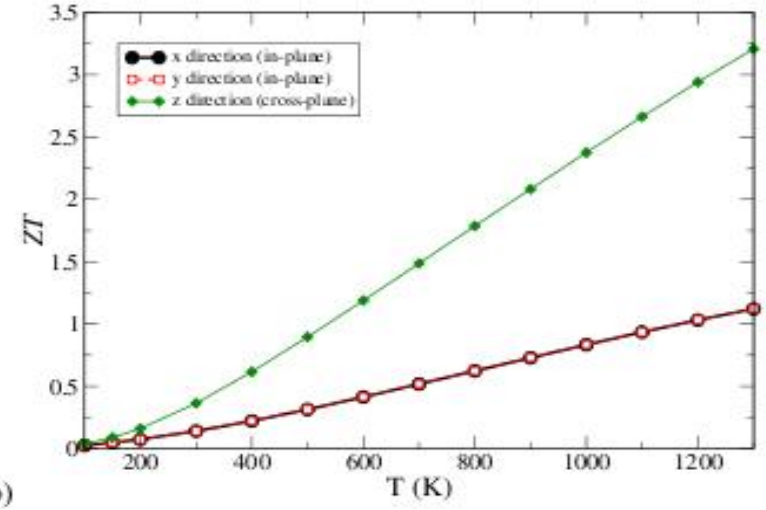

b)

ZT >3

Alloy and amorphous conductivity limits (~ 4 W/m/K) beaten

Thomas and Srivastava, AIP Conf Proc 1590, 95 (2014)

[3] Thin and thick PbTe-PbSe nanocomposites

PbSe nanoparticles inserted in PbTe host of sample size 500nm

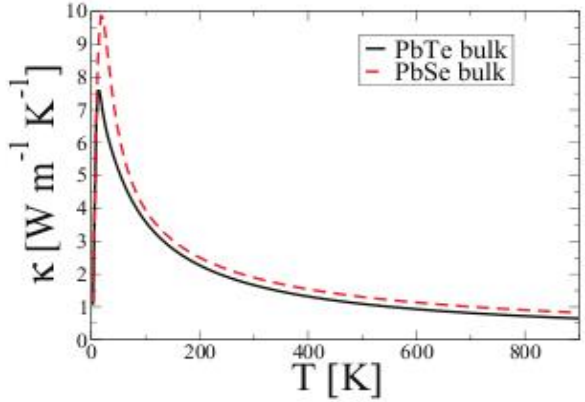

Figure 2. Lattice thermal conductivity results, computed using Callaway's expression, for bulk PbTe and PbSe samples in [34].

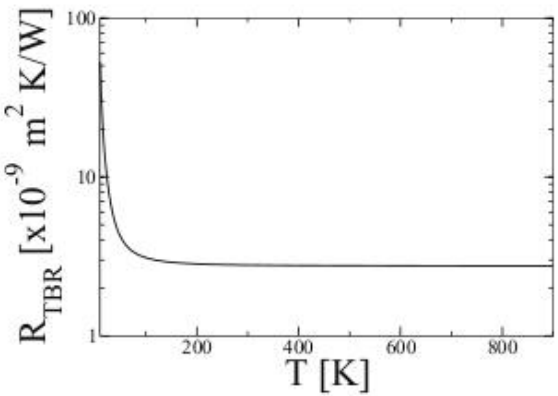

Figure 1. Temperature variation of the thermal boundary R_{TBR} resistance at the PbTe/PbSe interface.

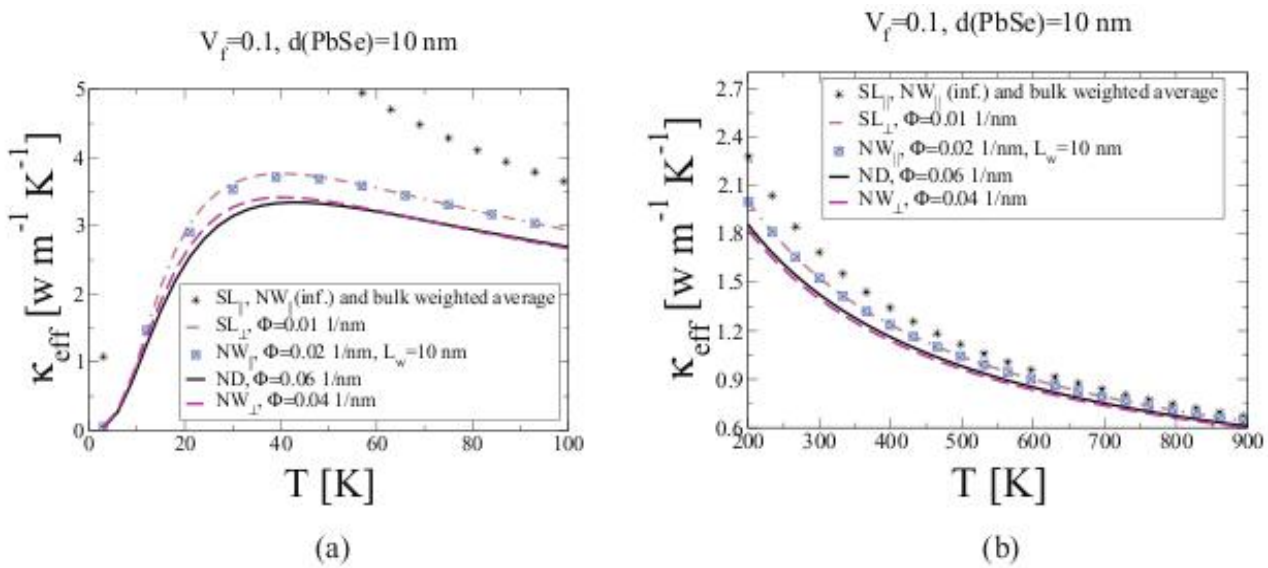

Figure 9. Effective thermal conductivity for different PbTe-PbSe nanocomposite configurations. Notice that the results along superlattice planes and along the axis of infinitely long nanowire are almost identical to the bulk weighted average result.

AlOtaibi and Srivastava. JPCM 28, 145304 (2016)

Dimensionality- and size-dependent phonon conductivity results for nanocomposites

- In general K(SL) > K(NW) or K(ND);
- For small nanodots (typically d=10 nm) K_{ph} is strongly influenced by interface density: $K_{ph} \propto 1/\sqrt{\Phi}$

AlOtaibi and Srivastava. JPCM 28, 145304 (2016)

Summary

- Discussed theoretical ingredients for tuning TE properties of semiconducting systems.

- Showed that the PGEC concept applied to nanocomposite structures has the potential to improve ZT in the range of commercial viability.

Acknowledgements

EPSRC (past support);
Leverhulme Trust (past and present support)

Steve Hepplestone; Iowerth Thomas

Ceyda Yelgel; Jawaher AlOtaibi

Thank you for listening

EXTRA SUPPLEMENTARY SLIDES

$$\kappa = \kappa_{el} + \kappa_{ph}$$

Normal practice:
Use free-electron Fermi gas model for calculating
S, σ and κ_{el}

$$\sigma = \frac{e\mu}{2\pi^2}\left(\frac{2kT}{\hbar^2}\right)^{3/2}\left(m_x m_y m_z\right)^{1/2} F_{1/2} \quad , \quad S = \frac{k}{e}\left(\frac{5F_{3/2}}{3F_{1/2}} - \zeta^*\right)$$

$$\kappa_e = \frac{\tau\hbar^2}{6\pi^2}\left(\frac{2kT}{\hbar^2}\right)^{5/2}\left(\frac{m_x m_y}{m_z}\right)^{1/2} k\left(\frac{7}{2}F_{5/2} - \frac{25F_{3/2}^2}{6F_{1/2}}\right)$$

$$\kappa = \kappa_e + \kappa_{ph} \quad , \quad F_i = F_i(\zeta^*) = \int_0^\infty \frac{x^i\,dx}{e^{(x-\zeta^*)} + 1}$$

Phys. Rev. B, L.D. Hicks, M.S. Dresselhaus, **47,**19,1993.

- For an n-type semiconductors

$$E_f = \frac{1}{2}(E_c + E_d) + \frac{k_b T}{2} \ln \frac{N_d}{2U_c} - k_b T \sinh^{-1}\left(\sqrt{\frac{U_c}{8N_d}} e^{-\frac{\Delta \epsilon_i}{2k_b T}}\right)$$

- For an intrinsic semiconductors

$$E_f = \frac{E_v + E_c}{2} + \frac{3}{4} k_b T \ln\left(\frac{m_p}{m_n}\right)$$

- Chemical potential

$$\zeta^* = \frac{E_f}{k_b T}$$

John P. McKelvey, Solid State and Semiconductor Physics, The Pennsylvania State University, 1966.

Phonon dispersion curves in bulk Si and Ge

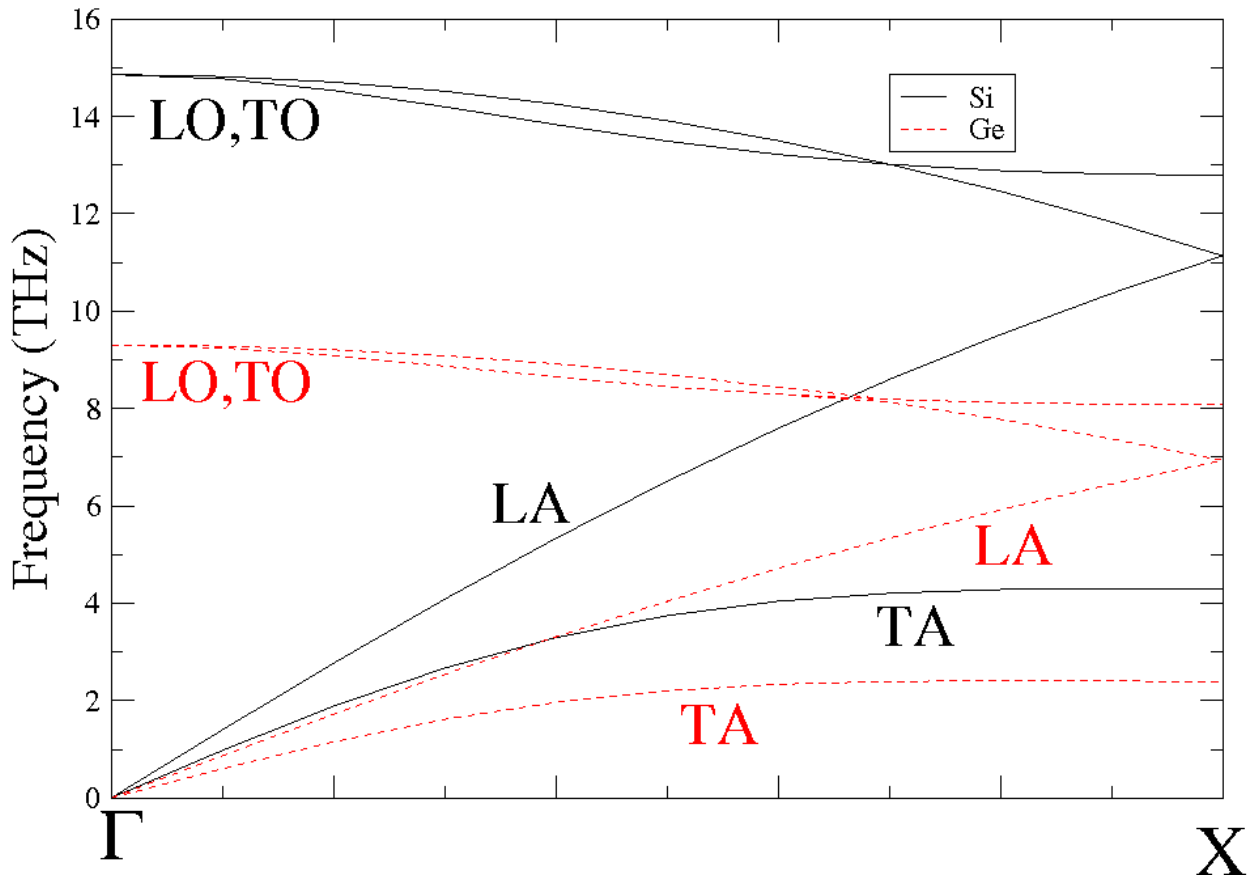

Results in complete agreement with experimental measurements

Interface mass-mixing scattering in A(n)/B(m) SLs

$$\tau_{\mathrm{IMS}}^{-1}(\boldsymbol{q}s) = \frac{\alpha\pi}{2N_0(n+m)^2}\int d\omega(\boldsymbol{q}'s')g(\omega(\boldsymbol{q}'s'))\omega(\boldsymbol{q}s)\omega(\boldsymbol{q}'s')$$
$$\times\frac{\bar{n}(\boldsymbol{q}'s')+1}{\bar{n}(\boldsymbol{q}s)+1}\delta(\omega(\boldsymbol{q}s)-\omega(\boldsymbol{q}'s')\left[(1-\frac{e_Ae'_A}{e_Be'_B})^2+(1-\frac{e_Be'_B}{e_Ae'_A})^2\right],$$

$g(\omega)$: density of states,

α : interface atomic mixing parameter,
e_B/e_A : interface atomic amplitude ratio.

$\tau = \tau(q, \omega$, amplitude ratio)

Interface broken-bonds scattering in A(n)/B(m) SLs

$$\tau_{\mathrm{IDS}}^{-1}(\boldsymbol{q}s) = \frac{\pi\omega_0^4}{4N_0}\frac{\alpha'}{(n+m)^2}\int d\omega(\boldsymbol{q}'s')\frac{g(\omega(\boldsymbol{q}'s'))}{\omega(\boldsymbol{q}s)\omega(\boldsymbol{q}'s')} \times\frac{\bar{n}(\boldsymbol{q}'s')+1}{\bar{n}(\boldsymbol{q}s)+1}\delta(\omega(\boldsymbol{q}s)-\omega(\boldsymbol{q}'s')) \times\left[1+\left(\frac{e_Ae'_A}{e_Be'_B}\right)^2+1+\left(\frac{e_Be'_B}{e_Ae'_A}\right)^2\right],$$

ω_0: highest phonon frequency,

α': parameter for concentration of broken bonds.

$\tau = \tau(q, \omega$, amplitude ratio)

Anharmonic scattering in SLs

$$\tau^{-1}(\boldsymbol{q}s) = \frac{\pi\hbar\rho_{av}^2\gamma^2}{N_0\Omega\bar{c}^2} \sum_{\boldsymbol{q}'s',\boldsymbol{q}''s'',\boldsymbol{G}} \omega(\boldsymbol{q}s)\omega(\boldsymbol{q}'s')\omega(\boldsymbol{q}''s'')DM(\boldsymbol{q}s,\boldsymbol{q}'s',\boldsymbol{q}''s'')$$
$$\times \left\{ \left[\frac{\bar{n}(\boldsymbol{q}'s')(\bar{n}(\boldsymbol{q}''s'')+1)}{\bar{n}(\boldsymbol{q}s)+1} \delta(\omega(\boldsymbol{q}s)+\omega(\boldsymbol{q}'s')-\omega(\boldsymbol{q}''s''))\delta_{\boldsymbol{q}+\boldsymbol{q}',\boldsymbol{q}''+\boldsymbol{G}} \right] \right.$$
$$\left. + \left[\frac{1}{2}\frac{\bar{n}(\boldsymbol{q}'s')\bar{n}(\boldsymbol{q}''s'')}{\bar{n}(\boldsymbol{q}s)} \delta(\omega(\boldsymbol{q}s)-\omega(\boldsymbol{q}'s')-\omega(\boldsymbol{q}''s''))\delta_{\boldsymbol{q}+\boldsymbol{G},\boldsymbol{q}'+\boldsymbol{q}''} \right] \right\},$$

ρ_{av} : average density of SL, $\bar{c}$: average acoustic velocity,

$\boldsymbol{G}$: reciprocal lattice vector $= 0$ ($\neq 0$) for Normal (Umklapp) processes,

γ : Grüneisen's constant.

$\tau = \tau(q, \omega, T, \text{amplitude ratio})$

Anharmonic scattering in A/B SLs -- Dual Mass Term

$$DM(\boldsymbol{q}s, \boldsymbol{q}'s', \boldsymbol{q}''s'') = \frac{1}{64}\{\frac{1}{2\rho_A^{\frac{3}{2}}}\times$$

$$\left[1 + \frac{\rho_A^{\frac{1}{2}}}{\rho_B^{\frac{1}{2}}}\left(\frac{e_B}{e_A} + \frac{e'_B}{e'_A} + \frac{e''_B}{e''_A}\right) + \frac{\rho_A}{\rho_B}\left(\frac{e_B e'_B}{e_A e'_A} + \frac{e'_B e''_B}{e'_A e''_A} + \frac{e_B e''_B}{e_A e''_A}\right) + \frac{\rho_A^{\frac{3}{2}}}{\rho_B^{\frac{3}{2}}}\left(\frac{e_B e'_B e''_B}{e_A e'_A e''_A}\right)\right] +$$

$$\frac{1}{2\rho_B^{\frac{3}{2}}}\left[1 + \frac{\rho_B^{\frac{1}{2}}}{\rho_A^{\frac{1}{2}}}\left(\frac{e_A}{e_B} + \frac{e'_A}{e'_B} + \frac{e''_A}{e''_B}\right) + \frac{\rho_B}{\rho_A}\left(\frac{e_A e'_A}{e_B e'_B} + \frac{e'_A e''_A}{e'_B e''_B} + \frac{e_A e''_A}{e_B e''_B}\right) + \frac{\rho_B^{\frac{3}{2}}}{\rho_A^{\frac{3}{2}}}\left(\frac{e_A e'_A e''_A}{e_B e'_B e''_B}\right)\right]\}^2$$

ρ = mass density

Phonon conductivity of short period Si/Ge superlattices

Theory of interface scattering and anharmonic interaction:
Originally by Hepplestone+GPS and revised by Thomas+GPS

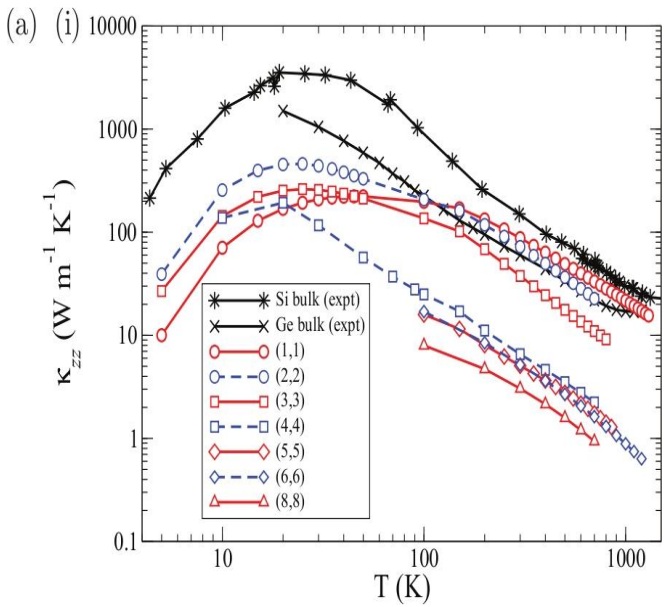

Si(n)/Ge(n)[001]
n=no. of bilayers

I Thomas and GPS
PRB 88, 115207 (2013)

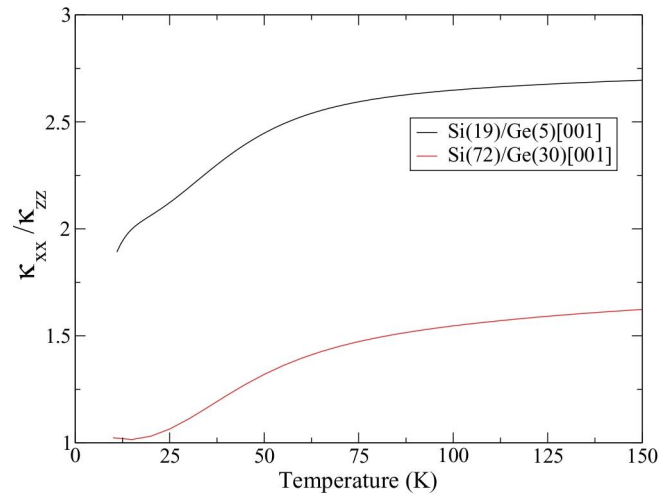

FIG. 11. (Color online) The thermal conductivity ratio κ_{xx}/κ_{zz} for the superlattices Si(19)/Ge(5)[001] and Si(72)/Ge(30)[001] as a function of temperature.

Si(n)/Ge(n)[001]
n=no. of monolayers

S P Hepplestone and GPS
PRB 84, 115326 (2011)

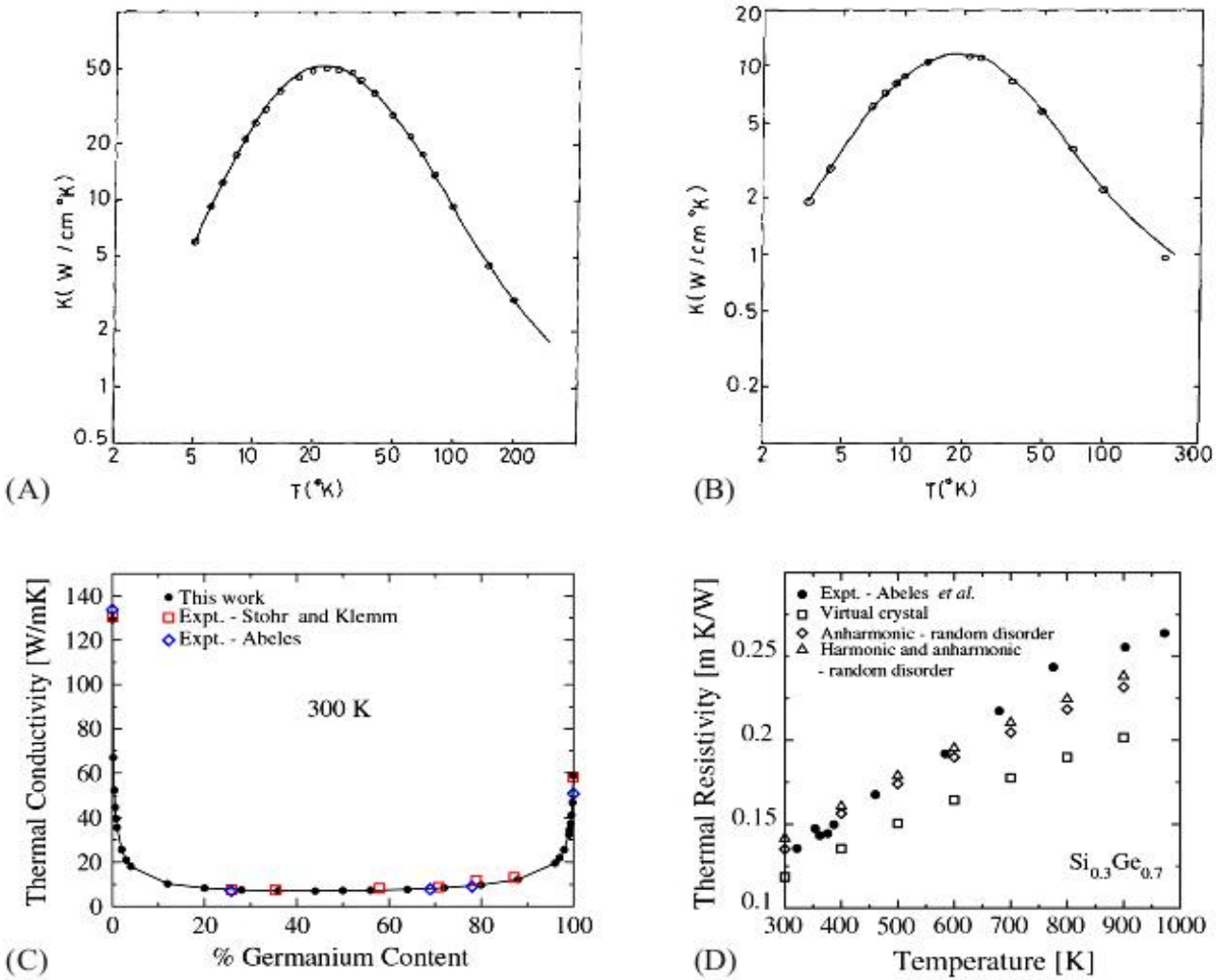

Figure 2 Lattice thermal conductivity of (A) Si (after Srivastava, 1980), (B) Ge (after Srivastava, 1980), (C) Si_xGe_{1-x} alloy at room temperature (after Garg *et al.*, 2011), and (D) $Si_{0.3}Ge_{0.7}$ alloy over a wide temperature range (after Garg *et al.*, 2011).

(A), (B): Srivastava, J Phys Chem Solids 41, 357 (1980)
(C), (D): Garg et al, PRL 106, 045901 (2011)

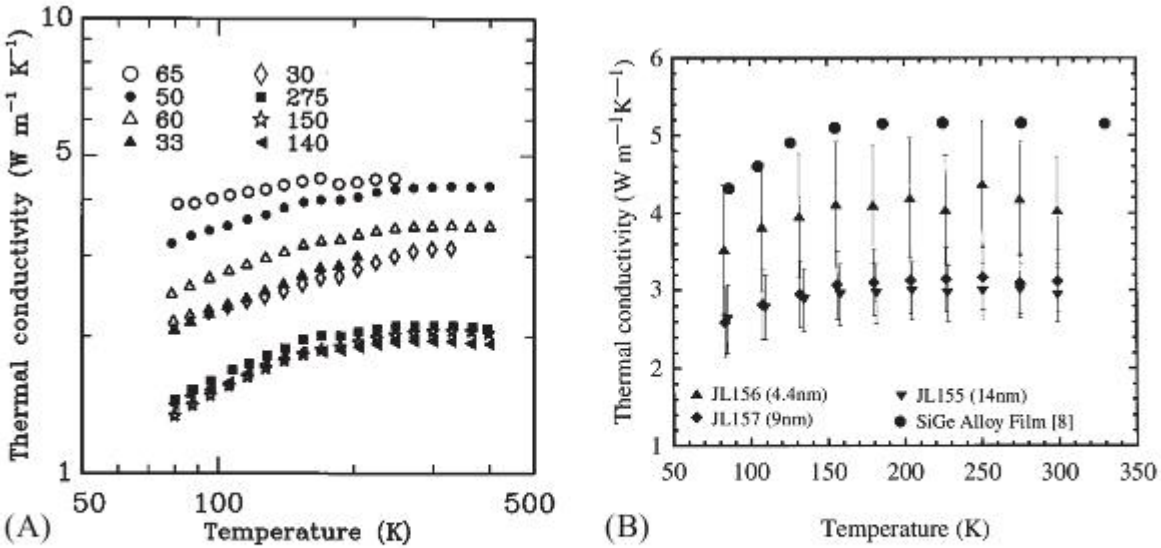

Figure 4 Cross-plane lattice thermal conductivity of SiGe alloy thin film and Si/Ge superlattices. Results in panel (A), from Lee *et al.* (1997), are for MOCVD grown *n* type samples ($n = 3 - 20 \times 10^{18}$ cm^{-3}) of total thickness in the range 0.9–1.8 μm and superlattice periodicty in the range 3.0–27.5 nm. Results in panel (B), from Borca-Tasciuc *et al.* (2000), are for undoped MBE grown superlattices with sample specifications [Si/Ge layer thicknesses in one period, total number of periods]: JL155 [(7 nm, 7 nm), 33]; JL156 [(2.2 nm, 2.2 nm), 100]; JL157 [(4.5 nm, 4.5 nm), 50]. Also shown in panel (B) are the results for a $Si_{0.85}Ge_{0.15}$ alloy film of thickness 1.14 μm and doping concentration $n = 3 \times 10^{18}$ cm^{-3}.

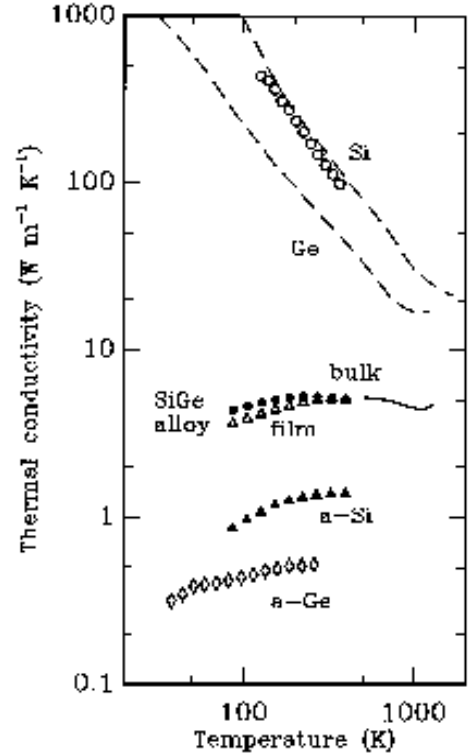

(A) and right-hand panel: Lee et al, APL 70, 2957 (1997)
(B): Borca-Tasciuc et al, Superlattice Microstr. 28, 199 (2000)